

Resistless Fabrication of Embedded Nanochannels by FIB Patterning, Wet Etching and Atomic Layer Deposition

Zhongmei Han, Marko Vehkamäki, Markku Leskelä and Mikko Ritala

Laboratory of Inorganic Chemistry, Department of Chemistry

University of Helsinki

Helsinki, Finland

E-mail: zhongmei.han@helsinki.fi

Abstract—Self-supported SiO_2 structures were fabricated from thermal SiO_2/Si substrates by combining FIB direct writing and selective and anisotropic chemical wet etching of silicon. These structures, such as SiO_2 overhangs on the edges of Si trenches, were then used as templates for ALD of Ta_2O_5 to form sealed nanochannels and cavities. The size of trenches formed by etching through openings in the SiO_2 increases with FIB patterning ion dose as well as KOH etching time. Channel formation results from sealing the trenches by the conformal ALD of Ta_2O_5 . The KOH etching time determines the channel size while the ion dose determines final wall thickness after ALD. The fabricated hollow nanochannels are embedded under SiO_2 and surrounded by Ta_2O_5 on crystalline Si. The channel size reaches 50 nm by this fabrication approach with a 60 min KOH etching time.

Keywords— nanochannels; focused ion beam; anisotropic etching; atomic layer deposition; SiO_2/Si

I. INTRODUCTION

Nanoscale channels are interesting nanostructures due to their promising applications such as filters, transistors, nanofluidics, and molecule sensors [1-4]. However, precise control of channel size and wall thickness is an issue for many nanochannel fabrication methods. Atomic layer deposition (ALD) is increasingly used in making 3D nanostructures due to the superior conformality and precise film thickness control [5, 6]. Ultra-thin films have been deposited by ALD on nanostructured templates such as nanopores [7-9], nanofibers [8, 10-12] and nanotubes [13, 14] for making 3D nanostructures. Furthermore, the deposited film materials can be selected depending on the application as many materials, including metals, oxides and nitrides, are available as ALD processes [6].

SiO_2 is an excellent insulating material and has been widely used in silicon-based devices for electrical and optical applications. Patterning of SiO_2 for various applications has been previously reported such as lift-off [15, 16], photolithography [17], electron beam lithography [18-20], reactive ion etching [21, 22], dynamical ploughing [23] and focused ion beam (FIB) direct writing [24, 25]. FIB direct writing is a maskless patterning technology for nanostructure fabrication [26]. In FIB systems, gallium is the mostly used

liquid metal ion source owing to its low melting point, commercial availability, and long lifetime. The main concern for FIB patterning is the Ga^+ implantation and damage to the target surface. However, majority of the gallium residue caused by FIB patterning of silicon can be removed by subsequent wet etching in a $\text{KOH}/\text{H}_2\text{O}_2$ solution at room temperature [27]. SiO_2 thin films can be grown easily on silicon wafers by thermal oxidation at high temperatures [28]. The thermal oxidation of silicon forms a stable and near-perfect SiO_2/Si interface [29]. In addition, the high etching selectivity between SiO_2 and Si in various etchants such as KOH and HF solutions makes wet etching also a patterning option for SiO_2/Si systems.

In this study, we combined FIB direct writing and chemical wet etching of silicon for nanofabrication of SiO_2 self-supported structures from thermal SiO_2 on Si substrates. The fabricated SiO_2/Si line trenches were used as a template for subsequent ALD of Ta_2O_5 to form embedded hollow nanochannels contacting with crystalline silicon. The resulting channels have a controllable width and height down to sub-100 nm. The fabrication process is illustrated in Fig. 1.

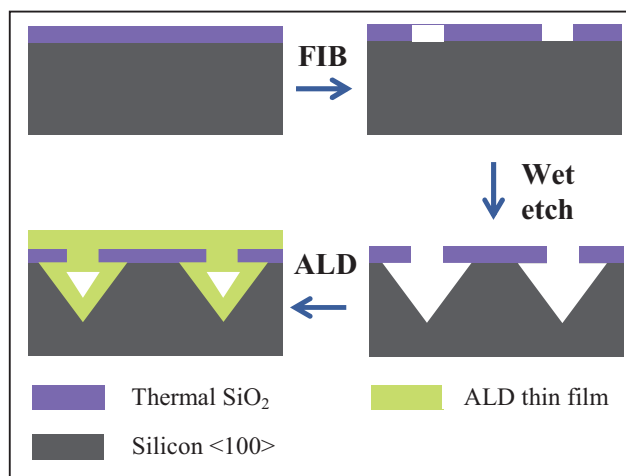


Fig. 1. Schematic illustration of fabrication steps (FIB patterning to open a line on the top SiO_2 , wet etching of Si under the SiO_2 layer, and ALD of conformal thin film) to form an embedded channel where the channel size, wall material and thickness are controllable.

II. EXPERIMENTAL

A. Fabrication of SiO_2 Structures

Silicon<100> wafers were thermally oxidized (1000 °C) to grow 105 nm thick SiO_2 films. The oxidized wafers were cleaved into small pieces (2 cm × 5 cm) which were then put into a FIB-SEM chamber for the direct writing by 30 keV gallium ion beam with 100 pA current and 90 % overlap. All the milled structures were aligned with the crystal structure by aligning the milled patterns parallel with the cleaved specimen edge. FIB patterned pieces were wet etched in three successive etching steps. 1 mol/L:1 mol/L KOH/ H_2O_2 solution was used immediately at room temperature for 3 hours to remove most of the gallium implanted layer and improve the thermal stability of the FIB patterned sites [27]. 1 % HF was used to remove native oxide and 1 mol/L KOH to etch the underlying silicon through the opened sites in SiO_2 and to release SiO_2 with the FIB patterned features.

B. ALD of Ta_2O_5 on SiO_2/Si Structures

ALD of Ta_2O_5 was subsequently performed on the FIB patterned and wet etched samples in a Microchemistry F-120 reactor at 250 °C with $\text{Ta}(\text{OEt})_5$ and water as precursors. Long purges were applied during the ALD process in order to remove the precursor vapors as well as possible from the almost-sealed channels.

III. RESULTS AND DISCUSSION

A. SiO_2 Structures Fabricated by FIB Patterning and Wet Etching

Si was etched from the FIB opened sites with KOH for 2 hours and suspended SiO_2 structures were formed due to the etching of Si below (Fig. 2). It is worth emphasizing that the removal of gallium residues with KOH/ H_2O_2 is critical for the use of the FIB patterned SiO_2 layer as a mask for the KOH wet etching of the underlying silicon – without the gallium removal the implanted gallium in silicon would stop or delay the following KOH etching process [27]. This method, combining FIB and wet etching, presents many options for preparing self-supported or hollow SiO_2 structures.

The FIB patterned structures were a circle ($d = 10 \mu\text{m}$), a ring ($d_{\text{outer}} = 20 \mu\text{m}$, $d_{\text{inner}} = 19.8 \mu\text{m}$), a square matrix ($a = 500 \text{ nm}$) and a line set on a SiO_2/Si piece before the chemical etching steps. The formed structures under SiO_2 shown in Fig. 2(a), (c) and (d) illustrate anisotropic etching of Si (100) and (111) planes while the Fig. 2(b) shows larger underetching resulting from much higher etching rate of (221) and (331) planes than (100) plane [30]. In Fig. 2(b), there is a large space under SiO_2 with a supporting pillar in the middle after the KOH etching of Si. The big membrane plate did not bend towards the bottom of etched Si in this case probably due to good stiffness of SiO_2 film and the anisotropic etching in diluted KOH (1 mol/L) at room temperature. After ALD of Ta_2O_5 on the etched SiO_2/Si , the SiO_2 plate was FIB cut to the middle to illustrate the cross section (Fig. 3) of the supporting pillar under the suspended SiO_2 plate in Fig. 2(b).

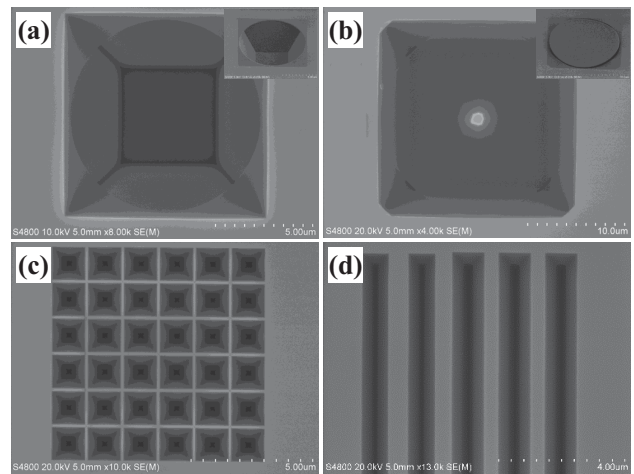


Fig. 2. SEM images of suspended SiO_2 structures made by etching with KOH for 2 h through different FIB patterned structures in the SiO_2 layer: (a) 10 μm -diameter circle, (b) 200 nm-wide ring (c) square matrix and (d) lines. Inset in (a) and (b) are corresponding tilted images with low voltage (3keV).

Templates for both nanochannels and microcavities can be prepared with this patterning approach, and interconnected networks of reservoirs and channels can be easily prepared with good control of both the size of the features and their relative placement. The ALD-covered membrane surfaces can be easily opened with FIB milling to produce gas or liquid

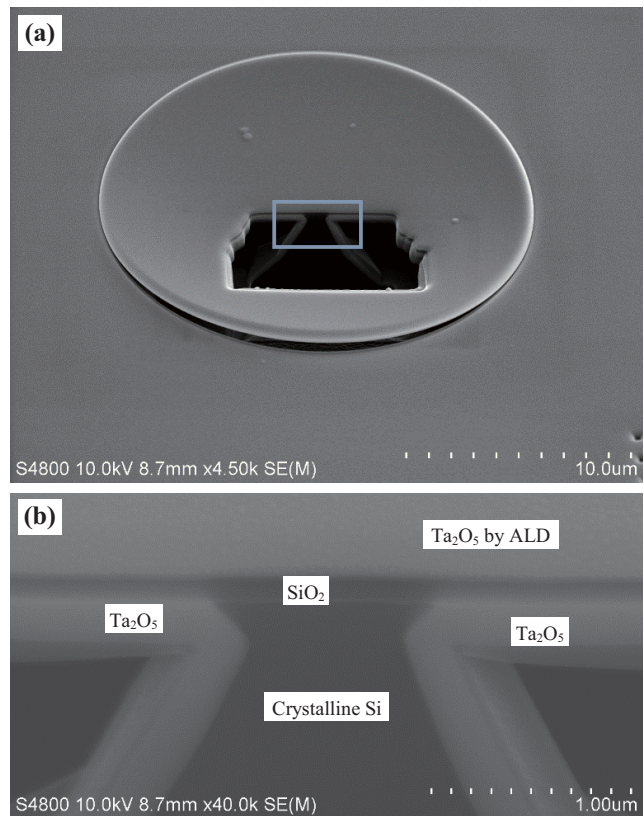


Fig. 3. (a) Cross sectional SEM image of plate-supporting pillar under the SiO_2 membrane shown in Fig. 2(b) after ALD of Ta_2O_5 , and (b) magnified image of the rectangular area in (a).

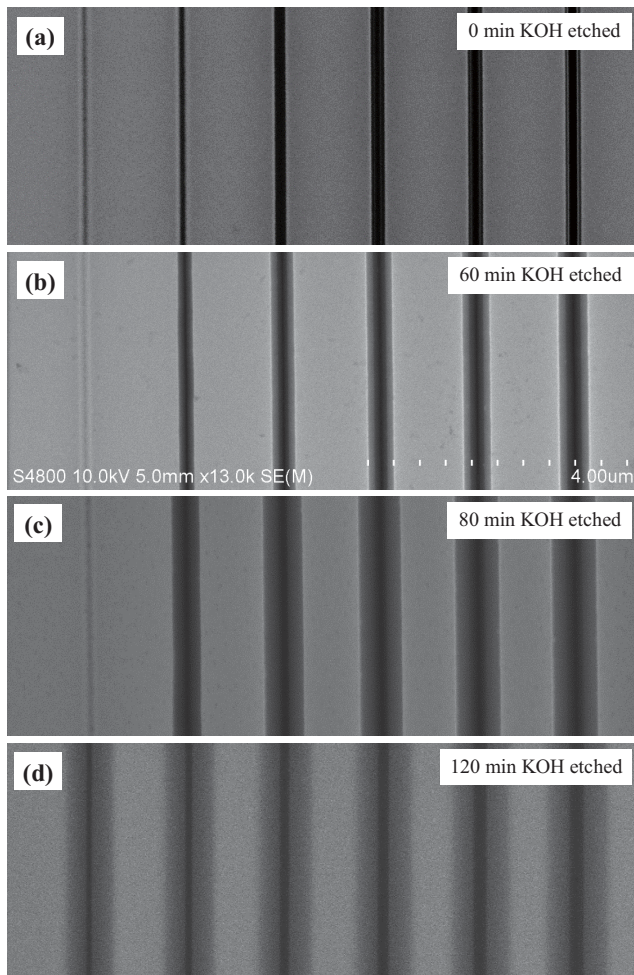


Fig. 4. SEM images of FIB patterned and wet etched line sets which were etched in KOH for (a) 0 min, (b) 60 min, (c) 80 min and (d) 120 min. The line separations were all set to 1.5 μm .

inlets of desired size, for example.

For line trenches, the patterning ion dose and KOH etching time are significant for the resulting trench size. Fig. 4 shows top-views of four line sets patterned by FIB with various ion doses followed by wet etching in the KOH etchant for 0, 60, 80 and 120 min, respectively. The lateral etch distance increases with etching time, but is independent of ion dose.

B. Nanochannel Formation with ALD

ALD Ta_2O_5 was chosen as the test material as it is amorphous, insulator, chemically stable and has high refractive index. After the FIB patterned line gaps were all closed by Ta_2O_5 film, cross sections were made by FIB milling. The SEM images in Fig. 5 show the channels formed after ALD of Ta_2O_5 thin film. The ion dose used for the FIB patterning increased from left to right in each image shown in Fig. 5, which results in larger opening in the SiO_2 layer. More ALD cycles were required for closing wider line gaps, resulting in thicker channel walls because the wall thickness equals to a half of the line gap.

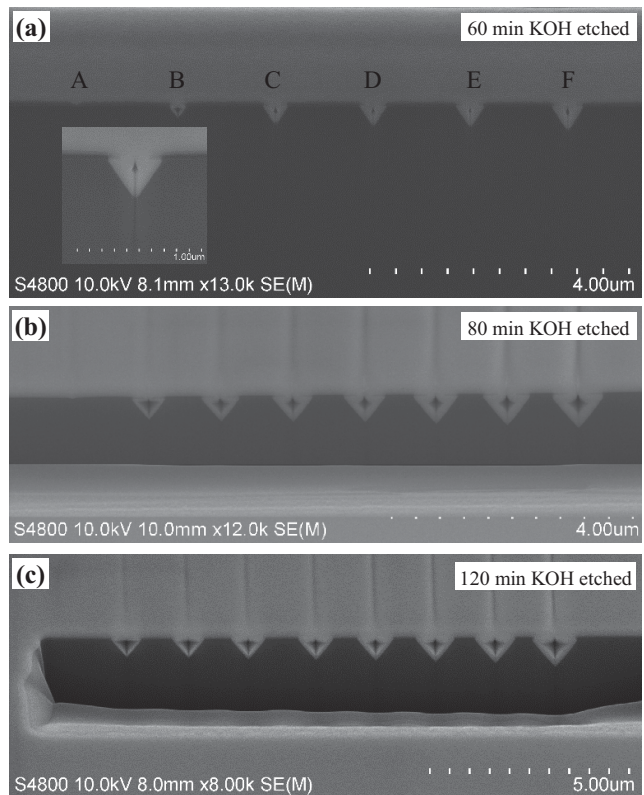


Fig. 5. Cross-section SEM images of nanochannels formed by FIB patterning, wet etching and ALD coating, corresponding to Fig. 4 (b), (c) and (d) respectively.

In Fig. 5(a), for example, the ion dose for line A made only a V-trench into SiO_2 but was not sufficient to reach the Si underneath. This prevented the wet etching of Si and thus did not result in suspended SiO_2 , so no channel was formed after ALD of Ta_2O_5 for line A. The patterning ion dose for line B was sufficient for exposing Si which could be etched in the KOH solution. More and more ion milling of Si occurred for lines C to F, which led to deeper line trenches after the KOH etching. Therefore, the ion dose controls both the size of line trenches before ALD and wall thickness of channels after ALD. Meanwhile, the KOH etching time determines the trench size and the resulting channel size. However the channel size for the same etching time does not vary significantly with the ion dose. By using ALD to form nanochannels, a wide variety of channel wall materials become available. One can also have different materials on the inside and outside the channel, if a bilayer or multilayer is deposited.

IV. CONCLUSIONS

This paper demonstrated a resistless fabrication method for embedded Ta_2O_5 channels by FIB direct writing, wet etching and ALD on SiO_2/Si substrates. The channel size is determined by KOH etching time and the wall thickness by the ion dose applied to make line opening into the SiO_2 layer. The wall materials can be selected depending on the application such as metals, oxides and nitrides as they are widely available in ALD processes, making this a highly versatile approach.

ACKNOWLEDGMENT

We wish to acknowledge financial support from China Scholarship Council (File No. 2011704017). We also gratefully acknowledge Finnish center of excellence in atomic layer deposition.

REFERENCES

- [1] R. Nagarajan, B. R. Murthy, and A. Linn, "Ultra-high aspect ratio buried silicon nano-channels for biological applications," *IEEE Sensors, Vols 1-3*, pp. 1276-1280, 2006.
- [2] I. J. Park, S. G. Jeon, and C. Shin, "A new slit-type vacuum-channel transistor," *IEEE Trans. Electron Devices*, vol. 61, pp. 4186-4191, Dec 2014.
- [3] H. Daiguji, P. D. Yang, and A. Majumdar, "Ion transport in nanofluidic channels," *Nano Lett.*, vol. 4, pp. 137-142, Jan 2004.
- [4] S. Howorka, S. Cheley, and H. Bayley, "Sequence-specific detection of individual DNA strands using engineered nanopores," *Nat. Biotechnol.*, vol. 19, pp. 636-639, Jul 2001.
- [5] M. Leskela and M. Ritala, "Atomic layer deposition chemistry: Recent developments and future challenges," *Angew. Chem. Int. Ed. Engl.*, vol. 42, pp. 5548-5554, Nov 2003.
- [6] V. Miiikkulainen, M. Leskelä, M. Ritala, and R. L. Puurunen, "Crystallinity of inorganic films grown by atomic layer deposition: Overview and general trends," *J. Appl. Phys.*, vol. 113, p. 021301, Jan 08 2013.
- [7] I. Perez, E. Robertson, P. Banerjee, L. Henn-Lecordier, S. J. Son, S. B. Lee, *et al.*, "TEM-based metrology for HfO₂ layers and nanotubes formed in anodic aluminum oxide nanopore structures," *Small*, vol. 4, pp. 1223-1232, Aug 2008.
- [8] M. Leskela, M. Kemell, K. Kukli, V. Pore, E. Santala, M. Ritala, *et al.*, "Exploitation of atomic layer deposition for nanostructured materials," *Mater. Sci. Eng., C*, vol. 27, pp. 1504-1508, Sep 2007.
- [9] M. Kemell, E. Harkonen, V. Pore, M. Ritala, and M. Leskela, "Ta₂O₅- and TiO₂-based nanostructures made by atomic layer deposition," *Nanotechnology*, vol. 21, p. 035301, Jan 2010.
- [10] M. Kemell, V. Pore, M. Ritala, M. Leskela, and M. Linden, "Atomic layer deposition in nanometer-level replication of cellulosic substances and preparation of photocatalytic TiO₂/cellulose composites," *JACS*, vol. 127, pp. 14178-14179, Oct 2005.
- [11] E. Santala, M. Kemell, M. Leskela, and M. Ritala, "The preparation of reusable magnetic and photocatalytic composite nanofibers by electrospinning and atomic layer deposition," *Nanotechnology*, vol. 20, p. 035602, Jan 2009.
- [12] E. Santala, J. Hamalainen, J. Lu, M. Leskela, and M. Ritala, "Metallic Ir, IrO₂ and Pt nanotubes and fibers by electrospinning and atomic layer deposition," *Nanosci. Nanotech. Lett.*, vol. 1, pp. 218-223, Dec 2009.
- [13] C. Marichy, N. Donato, M. Latino, M. G. Willinger, J. P. Tessonier, G. Neri, *et al.*, "Gas sensing properties and p-type response of ALD TiO₂ coated carbon nanotubes," *Nanotechnology*, vol. 26, p. 024004, Jan 2015.
- [14] S. H. Jin, G. H. Jun, S. H. Hong, and S. Jeon, "Conformal coating of titanium suboxide on carbon nanotube networks by atomic layer deposition for inverted organic photovoltaic cells," *Carbon*, vol. 50, pp. 4483-4488, May 2012.
- [15] T. Serikawa and T. Yachi, "Lift-off patterning of sputtered SiO₂-films," *J. Electrochem. Soc.*, vol. 128, pp. 918-919, 1981.
- [16] T. Yachi and T. Serikawa, "Lift-off patterning of sputtered SiO₂-films (lopas) and its application to recessed field isolation," *J. Electrochem. Soc.*, vol. 132, pp. 2775-2778, 1985.
- [17] C. Shafai, M. J. Brett, and T. M. Hrudehy, "Etch-induced stress failures of SiO₂ cantilever beams," *Sens. Actuators, A*, vol. 70, pp. 283-290, Oct 1998.
- [18] D. R. Allee and A. N. Broers, "Direct nanometer scale patterning of SiO₂ with electron-beam irradiation through a sacrificial layer," *Appl. Phys. Lett.*, vol. 57, pp. 2271-2273, Nov 1990.
- [19] P. E. Allen, D. P. Griffis, Z. J. Radzimski, and P. E. Russell, "Electron-beam patterning of SiO₂," *J. Vac. Sci. Technol., A*, vol. 10, pp. 965-969, Jul-Aug 1992.
- [20] J. W. Lussi, C. Tang, P. A. Kuenzi, U. Stauffer, G. Csucs, J. Voros, *et al.*, "Selective molecular assembly patterning at the nanoscale: A novel platform for producing protein patterns by electron-beam lithography on SiO₂/indium tin oxide-coated glass substrates," *Nanotechnology*, vol. 16, pp. 1781-1786, Jul 2005.
- [21] J. Q. Huang, Q. A. Huang, M. Qin, W. J. Dong, and X. W. Chen, "Experimental study on the dielectrostriction of SiO₂ with a micro-fabricated cantilever," *IEEE Sensors, Vols 1-3*, pp. 1030-1033, 2009.
- [22] K. Shimizu and S. Oda, "Fabrication of mos nanostructure by employing electron-beam lithography and anisotropic wet etching of silicon," *Jpn. J. Appl. Phys., Part 2*, vol. 30, pp. L415-L417, Mar 1991.
- [23] B. Klehn and U. Kunze, "SiO₂ and Si nanoscale patterning with an atomic force microscope," *Superlattices Microstruct.*, vol. 23, pp. 441-444, 1998.
- [24] S. W. Kim, T. Kotani, M. Ueda, S. Fujita, and S. Fujita, "Selective formation of Zn nanodots on nanopatterned substrates by metalorganic chemical vapor deposition," *Appl. Phys. Lett.*, vol. 83, pp. 3593-3595, Oct 2003.
- [25] M. Tanaka, K. Furuya, and T. Saito, "In-situ observation of focused ion beam micropatterns on semiconductors and insulators," *Jpn. J. Appl. Phys., Part 1*, vol. 37, pp. 7010-7014, Sept 1998.
- [26] C.-S. Kim, S.-H. Ahn, and D.-Y. Jang, "Review: Developments in micro/nanoscale fabrication by focused ion beams," *Vacuum*, vol. 86, pp. 1014-1035, Nov 2011.
- [27] Z. Han, M. Vehkamäki, M. Leskelä, and M. Ritala, "Selective etching of focused ion beam implanted regions from silicon as a nanofabrication method," *Nanotechnology*, vol. 26, p. 265304, Jun 2015.
- [28] B. E. Deal and A. S. Grove, "General relationship for thermal oxidation of silicon," *J. Appl. Phys.*, vol. 36, pp. 3770-3778, Dec 1965.
- [29] A. Pasquarello, M. S. Hybertsen, and R. Car, "Interface structure between silicon and its oxide by first-principles molecular dynamics," *Nature*, vol. 396, pp. 58-60, Nov 1998.
- [30] I. Zubel and I. Barycka, "Silicon anisotropic etching in alkaline solutions I. The geometric description of figures developed under etching Si(100) in various solutions," *Sens. Actuators, A*, vol. 70, pp. 250-259, Oct 1998.